Rocznik Ochrona Środowiska

Volume 25 Year 2023 ISSN 2720-7501 pp. 09-15

https://doi.org/10.54740/ros.2023.002 open access

Received: March 2023 Accepted: March 2023 Published: April 2023

Thermomechanical Homogenization in Steam Explosion

Anatoliy Pavlenko[1], Hanna Koshlak[2], Borys Basok[3], Tatiana Hrabova[4]*

[1]*Kielce University of Technology, Poland*
https://orcid.org/0000-0002-8103-2578
[2]*Kielce University of Technology, Poland*
https://orcid.org/0000-0001-8940-5925
[3]*Institute of Engineering Thermophysics of the National Academy of Sciences of Ukraine, Ukraine*
https://orcid.org/0000-0002-8935-4248
[4]*Institute of Engineering Thermophysics of the National Academy of Sciences of Ukraine, Ukraine*
https://orcid.org/0000-0002-5194-2474

[*]*corresponding author's e-mail:apavlenko@tu.kielce.pl*

Abstract: A steam explosion results from intense heat transfer when a thermolabile liquid phase comes into contact with a hot liquid. As a result of such contact, microdispersed fragmentation of a high-boiling liquid occurs. A mathematical model is proposed to describe the thermomechanical crushing process, considering the formation of a vapour layer at the interface between two phases and the force interaction concerning several simultaneously boiling particles of the dispersed phase.

Keywords: steam explosion, homogenisation, boiling

1. Effects of Intense Heat Transfer in Liquid Mixtures

When liquid mixtures, for example, emulsions, are heated to a temperature exceeding the boiling point of the low-boiling component at an appropriate pressure, the boiling of the thermolabile component may have the character of an explosion. In this case, a vapour layer appears at the interface between two liquids, which can increase in volume, collapse, and cause rapid fragmentation of the high-boiling component of the mixture of liquids (Albanese et al. 2019, Zevnik & Dular 2020). As the surface area between the liquids increases, fragmentation accelerates, rapidly increasing vapour pressure with explosive characteristics. The results of current experiments with liquid helium and water show that the rate of pressure increase can reach 1000 kPa/s (Ganesan et al. 2015, Chernin & Val 2017, Pham-Thanh et al. 2015, Dietzel et al. 2017). For explosive vaporisation, the key factors are the selection of optimal process parameters that will create conditions for fine fragmentation and determine the size of the resulting fragments (Pavlenko 2018, Pavlenko 2019, Warjito et al. 2021).

Some authors have proposed fragmentation models for superheated emulsions (Janssen & Kulacki 2017, Pavlenko 2020, Badv 2015) based on drop surface instability. At the same time, the fragmentation model can be described from the standpoint of thermodynamics because the process of forming a vapour film generates pressure pulses and creates significant gradients in the hydrodynamic parameters of the flow, which can cause droplets to break up to stable sizes.

This paper presents one of these approaches to assess the degree of dispersion of liquid mixtures during homogenisation.

2. Crushing of the Dispersed Phase During Emulsion Boiling

The classical theory of droplet deformation and destruction depending on the degree of flow turbulence belongs to Kolmogorov (Nigmatulin 2004), who considered this process a result of the manifestation of many random phenomena and, based on probability theory, obtained a logarithmic droplet size distribution. When considering these processes, the drop must resist the action of forces that tend to destroy it. The main factors determining the fragmentation of drops in a liquid medium are the relative velocity of the flow around the drop, flow acceleration, densities of the dispersed and continuous phases, surface tension, viscosities of both liquids and the characteristic time of their interaction. The types of hydrodynamic instability that arise under the influence of these factors will be as follows (Pavlenko et al. 2014a):

1) Tolmin-Schlichting instability resulting from the transition from laminar to turbulent flow.
2) Kelvin-Helmholtz instability occurs when two fluids move at different tangential velocities relative to the interface. When the flow is laminar, surface rupture can be observed even at low velocities. The Weber number characterises this type of instability:

$$We = \frac{2R\rho w^2}{\sigma}. \quad (1)$$

where R is the radius of the vapour bubble, w is the velocity of the vapour phase boundary, σ is the surface tension at the interface.

The critical Weber number equals $We_{cr} = 10$ (Pavlenko 2019).

3) Rayleigh-Taylor instability occurs if the surface between two fluids is accelerated from a lighter fluid to a heavier one. The Bond number characterises this type of instability:

$$Bo = \frac{4R^2\rho a}{\sigma}. \quad (2)$$

where a is the acceleration of the boundary motion.

The critical Bond number equals $Bo_{cr} = 40$ (Pavlenko 2019).

4) Benard's instability occurs due to density fluctuations, which consist of the fact that heavier layers are over lighter ones under the influence of certain causes (temperature gradient, concentration).

Tolmin-Schlichting and Benard's instabilities are observed in both homogeneous and heterogeneous systems, while Rayleigh-Taylor and Kelvin-Helmholtz-type instabilities are observed only in heterogeneous systems.

The calculations presented in the literature are mostly based on the Bond and Weber criteria (Pavlenko et al. 2014b, Tran et al. 2020, Adhikari et al. 2016, Chandrapala et al. 2012, Sun et al. 2020, Koshlak & Pavlenko 2019); i.e. consider only the Rayleigh-Taylor and Kelvin-Helmholtz instabilities, which are most characteristic of emulsion media. The processes of deformation and crushing of the dispersed phase (droplets) while moving in a liquid are described in (Prajapat et al. 2019, Merzkirch et al. 2015, Sun et al. 2021, Albanesea et al. 2019, Gasanov & Bulanov 2015, Dąbek et al. 2016, Dąbek et al. 2018). At the same time, no existing model considers the process of fragmentation of the dispersed phase, taking into account the formation of a vapour layer at the interface between two phases and the force interaction with respect to several simultaneously boiling particles of the dispersed phase. The possible processes of deformation and crushing under the influence of either explosive boiling, the growth of steam bubbles, or the impact of steam caverns, cavitation cavities at the moment of their collapse, when the most significant dynamic effect is possible, are described. A vapour cavity (bubble) formation is assumed to be homogeneous, and only the maximum dynamic effects are considered. At the same time, the destruction of the dispersed phase can occur at any other time because the hydrodynamic situation in the vicinity of two growing bubbles is uncertain. If a particle of the dispersed phase is located at some distance from these bubbles (or between them at a certain distance), then the effect of fragmentation of this particle will manifest itself upon reaching the maximum force, which will exceed the critical one calculated according to the Weber or Bond criteria, but will not necessarily be equal to the maximum that can act in this system. If we consider the thermomechanical crushing of the dispersed phase, which boils, the process becomes even more complex and requires a detailed study.

The main factors that determine the crushing of the dispersed phase are shown above. According to the criteria of Weber and Bond, the main factors determining the fragmentation of the dispersed phase, respectively, will be the speed (relative velocity) w and the acceleration a, acting on a given (dispersed) particle. The speed at any point in space in the vicinity of a growing or collapsing vapour volume (bubble) can be determined by the relation:

$$w(r) = \frac{wR^2}{r^2}, \quad (3)$$

where r is the radius of a drop of a low-boiling liquid.

It can be seen from this relationship that this velocity is inversely proportional to the square of the radius (starting from the value of the radius of the vapour volume itself).

The distribution of acceleration in the vicinity of the bubble is determined (described) by the expression:

$$g(r,\tau) = \left(p - p_\infty + 0.5w^2\rho \ - \frac{2\rho\ w^2R^3}{r^3} \right) \frac{R}{\rho\ r^2}, \quad (4)$$

where:

τ – time,

p – pressure in the vapour phase,

$p\infty$ – pressure in the liquid mixture,

ρ – density of the high-boiling liquid.

The results of calculations for the dispersed system "vapour-liquid" according to equation (5) are shown in Fig. 1.

As can be seen from this figure, the acceleration at certain points in time depends ambiguously on the distance r: it can have a negative value at the oil-steam interface, increase with increase r and, having reached a maximum, decrease, even at a distance four times the radius of the drop, the acceleration is many times greater than the acceleration due to gravity. From this, we can conclude that a dispersed phase drop located at a distance several times greater than the radius of a boiling particle is subjected to accelerations that cause a destabilising effect of this drop and, under certain parameters (R, σ, g), can destroy it.

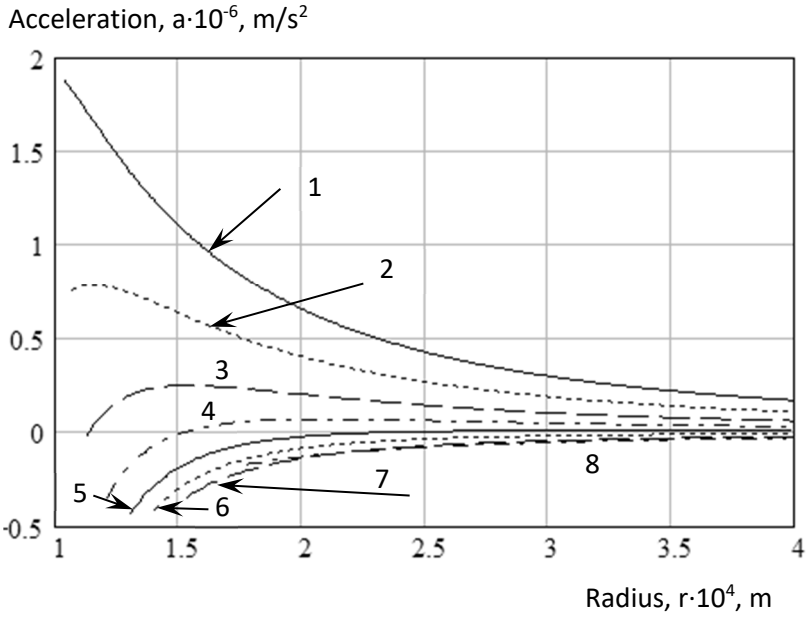

Fig. 1. Distribution of acceleration in the vicinity of the vapour layer during its growth for R = 200 μm, t = 170°C as a result of pressure drop to 1 bar, at different times: 1 – 10^{-6} s; 2 – $1.5 \cdot 10^{-6}$ s; 3 – $2.4 \cdot 10^{-6}$ s; 4 – $3.6 \cdot 10^{-6}$ s; 5 – $5.2 \cdot 10^{-6}$ s; 6 – $7 \cdot 10^{-6}$ s; 7 – 10^{-5} s; 8 – $2 \cdot 10^{-6}$ s

Let us consider a system consisting of two drops of different sizes when they boil due to pressure release located at a distance from each other (Fig. 2).

The formula (5) determines the resulting acceleration of the vapour layer boundary

$$g(x,\tau) = \sum_{i=1}^{2} \left(p - p_{\infty} + 0.5\rho\, w^2 - \frac{2\rho\, w^2 R^3}{r_i^3} \right) \frac{(x_i - x)R_i}{r_i^3}, \tag{5}$$

where x_i are the initial coordinates of the drop centres; $d = |x_i - x|$ is the radius vector; x is the coordinate of the acceleration determination point; w_i is the speed of movement of the oil-steam interface for the i-th drop; R_i is the radius of the oil-vapor interface of the i-th drop.

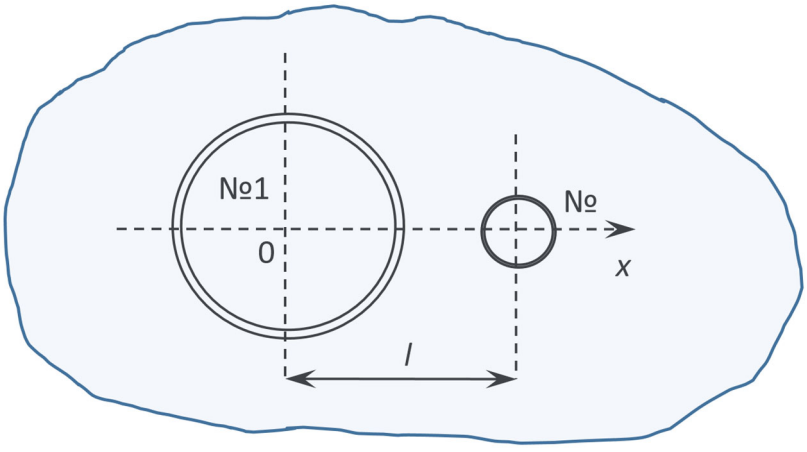

Fig. 2. Calculation scheme for the arrangement of drops

The results of calculations for two bubbles in a liquid are presented in Fig. 3. It follows from the above figure that the acceleration field can change dramatically depending on the distance between the particles, up to a complete change in the direction of the acceleration vector and, as a consequence, the possible destruction of any of the particles.

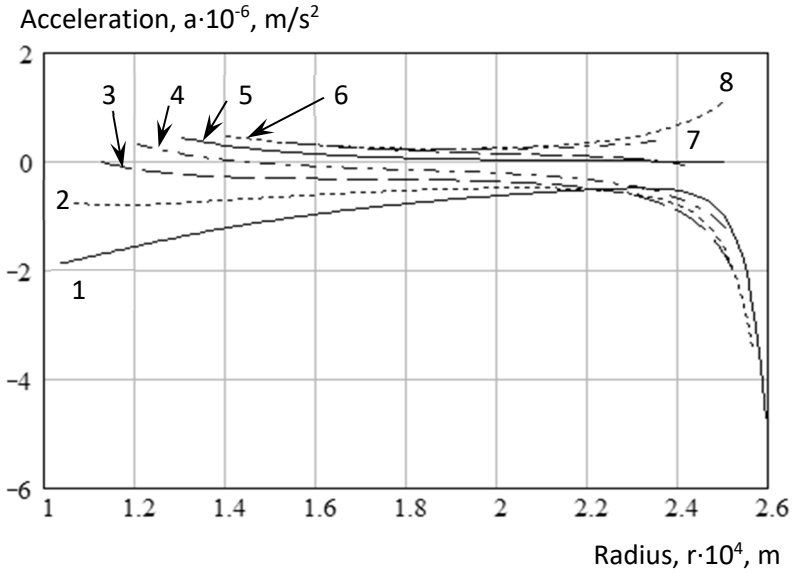

Fig. 3. Acceleration distribution between two growing vapour volumes at different times (notation from Fig. 2). d = $3 \cdot 10^{-4}$ m, R_1 = 100 μm, R_2 = 10 μm, t = 170°C as a result of pressure drop to 1 atm, at different time points: 1 – 10^{-6} s; 2 – $1.5 \cdot 10^{-6}$ s; 3 – $2.4 \cdot 10^{-6}$ s; 4 – $3.6 \cdot 10^{-6}$ s; 5 – $5.2 \cdot 10^{-6}$ s; 6 – $7 \cdot 10^{-6}$ s; 7 – 10^{-5} s; 8 – $2 \cdot 10^{-6}$ s

It is clear that equation (5) does not consider the vortex flows that arise in the space between the vapour volumes of the drops given their complete uncertainty.

Fig. 4 shows the joint graphs of the change in the velocity of the liquid-vapour interface and its acceleration at the initial temperature of the system t = 170°C for different initial droplet radii.

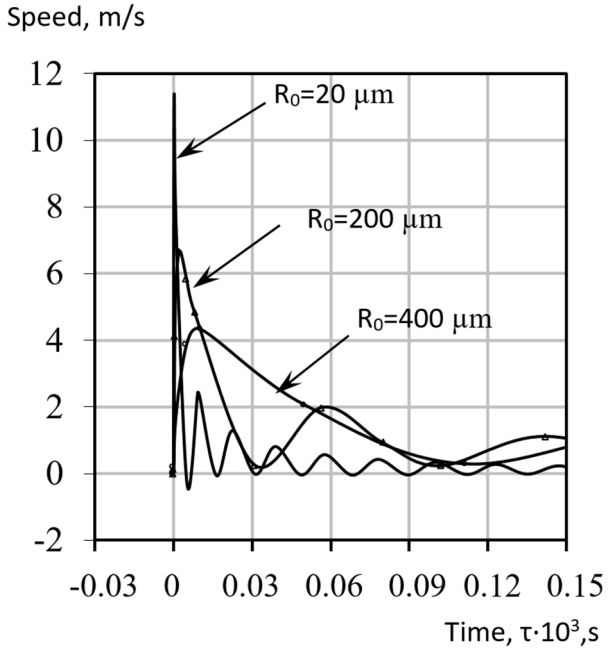

Fig. 4. General graph of the change in the movement of the liquid-vapour interface for various initial droplet radii

It can be seen from these graphs that the smaller the initial droplet radius, the more intensively the vapour phase will grow, i.e. higher speed and acceleration of the movement of the phase boundary. At different

droplet radii, both general velocities (minimum) and significant differences in these velocities (accelerations) can be observed.

Then, when it is assumed that the velocities (accelerations) for different initial radii have different amplitudes and frequencies of change in time, it can be assumed that at some point in time the Kelvin-Helmholtz instability may occur, and for acceleration the Rayleigh-Taylor instability.

Let us define the force interaction, which can lead to the appearance of this or that instability. From the joint consideration of the Bond and Weber criteria, as well as their critical values, with the Rayleigh-Plesset equation, it follows that the essential forces leading to the appearance of the Rayleigh-Taylor or Kelvin-Helmholtz instability, respectively, are equal to

$$F_{Bo}^{cr} = 40\pi\sigma R, \tag{6}$$

$$F_{We}^{cr} = 30\pi\sigma R. \tag{7}$$

A comparison of (6) and (7) shows that $F_{Bo}^{cr} = 1.33F_{We}^{cr}$, but these forces are caused by different factors and cannot be identified.

Deformation and crushing of both the vapour layer and the water drop in emulsions, for example, of the water-oil type, can be caused by different directions of both the acceleration vector and the velocity vector. We assume that deformation, crushing, or displacement will occur only if the acceleration vector has a positive direction and, regardless of it, the velocity vector is also positive. We will assume that the coordinates of drop No. 1 (Fig. 2) and drop No. 2 are equal $x_1 = 0$, $x_2 = d$.

We make the following assumptions:

1) no matter how great the acceleration or velocity of the boundary of the particle itself is, the possible instabilities caused by them cannot destroy the given boundary of the particle;

2) if the interface's acceleration (velocity) vector is unidirectional with the acceleration vector acting on the particle boundary from the neighbouring side, then the resulting vector is equal to the one acting on the boundary from the adjacent side.

Taking into account these assumptions, the expression (5) for acceleration, which tends to destroy the interface of droplet No. 1, has the form:

$$a = \begin{cases} \sum_{i=1}^{2} a_1;\ k_1 \geq 0, k_2 \geq 0, \\ -\sum_{i=1}^{2} a_2;\ k_1 \leq 0, k_2 \leq 0, \\ a_2;\ k_1 < 0, k_2 > 0, \\ -a_2;\ k_1 > 0, k_2 < 0, \end{cases} \tag{8}$$

where:

$$a_i = \left(p - p_\infty + 0.5 w_i^2 \rho - \frac{2\rho\, w_i^2 R_i^3}{r_i^3} \right) \frac{R_i (x_i - R_1)}{\rho \cdot r_i^3};$$

$$k_i = p - p_\infty + 0.5 w_i^2 \rho - \frac{2\rho\, w_i^2 R_i^3}{r_i^3};\ d_i = |x_i - R_1|.$$

Then the force caused by the acceleration or deceleration of the flow is equal to

$$F_{Bo_1} = 4\pi\rho\, a_1 R_1^3. \tag{9}$$

Similarly, we can write for speed:

$$w_i = \begin{cases} \sum_{i=1}^{2} w_{r_i};\ w_1 \geq 0, w_2 \geq 0, \\ -\sum_{i=1}^{2} w_{r_i};\ w_1 \leq 0, w_2 \leq 0, \\ w_{r_2};\ w_1 < 0, w_2 > 0, \\ -w_{r_2};\ w_1 > 0, w_2 < 0, \end{cases} \tag{10}$$

where:

$$w_{r_i} = w_i R_i^2 \frac{|x_i - R_1|}{r_i^3}.$$

Then the force of the dynamic head:

$$F_{We_1} = 6\pi\rho\, R_1^2 |w_1| w_1. \tag{11}$$

As is known, the capillary force $F\sigma$, regardless of the shape of the deformed drop, is always directed in such a way as to restore the spherical shape, i.e. to keep the Gibbs surface energy to a minimum. Therefore, if the drop deforms into an oblate ellipsoid in the direction of its motion, the capillary force counteracts the external force. If it is deformed into an elongated ellipsoid, then the capillary force coincides in the direction with the external force. Hence it follows that an elongated ellipsoid's shape is unstable during deformation, while the shape of an oblate ellipsoid can be quasi-stable.

There may be a minimum of this capillary force. We will assume that the Laplace force determines this minimum and the corresponding force is equal to:

Thus, when the external force exceeds the force F_σ, the given volume will be crushed, if the forces are equal, equilibrium will occur, and if $F_\sigma > F_{Bo,We}$, the given volume will be repulsed without deformation.

3. Conclusions

The study of the phenomena of explosive boiling of a liquid in relation to its directed and effective use to stimulate and intensify technological processes requires a unified approach that equally considers the hydrodynamic and heat and mass transfer aspects of these phenomena. Within the framework of this concept, we propose a new method for assessing boiling kinetics. This technique is based on a modernised model that, considering all the determining factors and an accurate representation of the thermophysical system parameters, adequately describes the behaviour of bubbles in boiling processes.

Approbation of the technique was carried out on an example of the boiling of an overheated emulsion with a sharp decrease in pressure. At the interface between the liquid phases, vapour fluids are formed, the volume of which rapidly increases. Thus, conditions for the occurrence of dynamic effects on the structure of the emulsion (liquid mixtures) are created. Moreover, the level of this effect can be easily controlled using the temperature and pressure of preheating the emulsion.

This study should be considered the initial stage in substantiating the rational homogeniser design in solving various technological problems.

References

Adhikari, Ram, Chandra, Vaz, Jerson, Wood, D. (2016). Cavitation Inception in Cross-Flow Hydro Turbines. *Energies*, *9*(4), 237. https://doi.org/10.3390/en9040237

Albanese, L., Baronti, S., Liguori, F., Meneguzzo, F., Barbaro, P., Vaccari, F.P. (2019). Hydrodynamic cavitation as an energy-efficient process to increase biochar surface area and porosity: A case study. *Journal of Cleaner Production*, *210*, 159-169. https://doi.org/10.1016/j.jclepro.2018.10.341

Badve, M.P., Alpar, T., Pandit, A.B., Gogate, P.R., Csoka, L. (2015). Modeling the shear rate and pressure drop in a hydrodynamic cavitation reactor with experimental validation based on KI decomposition studies. *Ultrasonics Sonochemistry*, *22*, 272-277. https://doi.org/10.1016/j.ultsonch.2014.05.017

Bao, Ngoc, Tran, Haechang, Jeong, Jun-Ho, Kim, Jin-Soon, Park, Changjo, Yang, (2020). Effects of Tip Clearance Size on Energy Performance and Pressure Fluctuation of a Tidal Propeller Turbine. *Energies*, *13*, 4055. https://doi.org/10.3390/en13164055

Chandrapala, J., Oliver, C., Kentish, S., Ashokkumar, M. (2012). Ultrasonics in food processing – food quality assurance and food safety. *Trends in Food Science & Technology*, *26*(2), 88-98. https://doi.org/10.1016/j.tifs.2012.01.010

Chernin, Leon, Dimitri, V.Val. (2017). Probabilistic prediction of cavitation on rotor blades of tidal stream turbines. *Renewable Energy*, *113*, 688-696. https://doi.org/10.1016/j.renene.2017.06.037

Dąbek, L., Kapjor, A., Orman, Ł.J. (2016). *Ethyl alcohol boiling heat transfer on multilayer meshed surfaces*. Proc. of 20th Int. Scientific Conference on The Application of Experimental and Numerical Methods in Fluid Mechanics and Energy 2016, AIP Conference Proceedings, 1745, 020005. https://doi.org/10.1063/1.4953699

Dąbek, L., Kapjor, A., Orman, Ł.J. (2018). *Boiling heat transfer augmentation on surfaces covered with phosphor bronze meshes*. Proc. of 21st Int. Scientific Conference on The Application of Experimental and Numerical Methods in Fluid Mechanics and Energy 2018, MATEC Web of Conferences, 168, 07001. https://doi.org/10.1051/matecconf/201816807001

Dietzel, Dirk, Hitz, Timon, Munz, Claus-Dieter, Kronenburg, Andreas, (2017). *Expansion rates of bubble clusters in superheated liquids*. Polytechnic University of Valencia Congress, ILASS2017. 28th European Conference on Liquid Atomization and Spray Systems, 6-8 September 2017, Valencia, Spain. http://dx.doi.org/10.4995/ILASS2017.2017.4714

Feng, Jie, Muradoglu, Metin, Kim, Hyoungsoo, Ault, Jesse, T., Stone, Howard, A. (2016). Dynamics of a bubble bouncing at a liquid/liquid/gas interface. *Journal of Fluid Mechanics*, *807*, 324-352. https://doi.org/10.1016/j.ultrasmedbio.2005.02.007

Ganesan, Balasubramanian, Martini, Silvana, Solorio, Jonathan, Walsh, Marie, K. (2015). Determining the Effects of High Intensity Ultrasound on the Reduction of Microbes in Milk and Orange Juice Using Response Surface Methodology. *International Journal of Food Science*, *2015*, Article ID 350719. https://doi.org/10.1155/2015/350719

Gasanov, B.M., Bulanov, N.V. (2015). Effect of the droplet size of an emulsion dispersion phase in nucleate boiling and emulsion boiling crisis. *International Journal of Heat and Mass Transfer*, *88*, 256-260. https://doi.org/10.1016/j.ijheatmasstransfer

Janssen, D., Kulacki, F.A. (2017). Flow boiling of dilute emulsions. *International Journal of Heat and Mass Transfer*, *115*, Part A, 1000-1007. https://doi.org/10.1016/j.ijheatmasstransfer.2017.07.093

Koshlak, H., Pavlenko, A. (2019). Method of formation of thermophysical properties of porous materials. *Rocznik Ochrona Srodowiska*, *21*(2), 1253-1262.

Merzkirch, W., Rockwell, D., Tropea, C. (2015). *Orifice Plates and Venturi Tubes*. Cham; Heidelberg; New York, NY; Dordrecht; London: Springer International Publishing. Available online at: https://link.springer.com/content/pdf/bfm%3A978-3-319-16880-7%2F1.pdf

Nhut, Pham-Thanh, Hoang, Van, Tho, Young, Jin, Yum. (2015). Evaluation of cavitation erosion of a propeller blade surface made of composite materials. *Journal of Mechanical Science and Technology*, *29*, 1629-1636.

Nigmatulin, R., Taleyarkhan, R., Lahey, R. (2004). Evidence for nuclear emissions during acoustic cavitation revisited. *Journal of Power and Energy*, *218*, Part A: J. Power and Energy. https://doi.org/10.1243/0957650041562208

Pavlenko, A., Koshlak, H., Usenko, B. (2014a). The processes of heat and mass exchange in the vortex devices. *Metallurgical and Mining Industry*, *6*(3), 55-59.

Pavlenko, A., Koshlak, H., Usenko, B. (2014b). Heat and mass transfer in fluidised layer. *Metallurgical and Mining Industry*, *6*(6), 96-100.

Pavlenko, A.M. (2018). Dispersed phase breakup in boiling of emulsion. *Heat Transfer Research*, *49*(7), 633-641, https://doi.org/10.1615/HeatTransRes.2018020630

Pavlenko, A.M. (2019). Energy conversion in heat and mass transfer processes in boiling emulsions. *Thermal Science and Engineering Progress*, *15*, 1-8. https://doi.org/10.1016/j.tsep.2019.100439

Pavlenko, A.M., Koshlak, H. (2021). Application of thermal and cavitation effects for heat and mass transfer process intensification in multicomponent liquid media. *Energies*, *14*(23), 7996. https://doi.org/10.3390/en14237996

Prajapat, A.L., Gogate, P.R. (2019). Depolymerisation of carboxymethyl cellulose using hydrodynamic cavitation combined with ultraviolet irradiation and potassium persulfate. *Ultrasonics Sonochemistry*, *51*, 258-263. https://doi.org/10.1016/j.ultsonch.2018.10.009

Sun, X., Wang, Z., Xuan, X., Ji, L., Li, X., Tao, Y., Boczkaj, G., Zhao, S., Yoon, J.Y., Chen, S. (2021). Disinfection characteristics of an advanced rotational hydrodynamic cavitation reactor in pilot scale. *Ultrasonics Sonochemistry*, *73*, 105543. https://doi.org/10.1016/j.ultsonch.2021.105543

Xun, Sun, Songying, Chen, Jingting, Liu, Shan, Zhao, Joon, Yong, Yoon. (2020). Hydrodynamic Cavitation: A Promising Technology for Industrial-Scale Synthesis of Nanomaterials. *Front. Chem.*, *15*. https://doi.org/10.3389/fchem.2020.00259

Zevnik, Jure, Dular, Matevž, (2020). Cavitation bubble interaction with a rigid spherical particle on a microscale. *Ultrasonics Sonochemistry*, *69*, 105252. https://doi.org/10.1016/j.ultsonch.2020.105252